Acta Oceanol. Sin., 2013, Vol. 32, No. 10, P. 48-56
DOI: 10.1007/s13131-013-0365-6
http://www.hyxb.org.cn
E-mail: hyxbe@263.net

Optical detection of *Prorocentrum donghaiense* blooms based on multispectral reflectance

TAO Bangyi[1], PAN Delu[1]*, MAO Zhihua[1], SHEN Yuzhang[1], ZHU Qiankun[1], CHEN Jianyu[1]

[1] State Key Laboratory of Satellite Ocean Environment Dynamics, Second Institute of Oceanography, State Oceanic Administration, Hangzhou 310012, China

Received 1 February 2013; accepted 29 March 2013

Abstract
Prorocentrum donghaiense is one of the most common red tide causative dinoflagellates in the Changjiang (Yangtze) River Estuary and the adjacent area of the East China Sea. It causes large-scale blooms in late spring and early summer that lead to widespread ecologic and economic damage. A means for distinguishing dinoflagellate blooms from diatom (*Skeletonema costatum*) blooms is desired. On the basis of measurements of remote sensing reflectance [$R_{rs}(\lambda)$] and inherent optical parameters, the potential of using a multispectral approach is assessed for discriminating the algal blooms due to *P. donghaiense* from those due to *S. costatum*. The behavior of two reflectance ratios [$R_1 = R_{rs}(560)/R_{rs}(532)$ and $R_2 = R_{rs}(708)/R_{rs}(665)$], suggests that differentiation of *P. donghaiense* blooms from diatom bloom types is possible from the current band setup of ocean color sensors. It is found that there are two reflectance ratio regimes that indicate a bloom is dominated by *P. donghaiense*: (1) $R_1 > 1.55$ and $R_2 < 1.0$ or (2) $R_1 > 1.75$ and $R_2 \geqslant 1.0$. Various sensitivity analyses are conducted to investigate the effects of the variation in varying levels of chlorophyll concentration and colored dissolved organic matter (CDOM) as well as changes in the backscattering ratio (b_{bp}/b_p) on the efficacy of this multispectral approach. Results indicate that the intensity and inherent optical properties of the algal species explain much of the behavior of the two ratios. Although backscattering influences the amplitude of $R_{rs}(\lambda)$, especially in the 530 and 560 nm bands, the discrimination between *P. donghaiense* and diatoms is not significantly affected by the variation of b_{bp}/b_p. Since $a_{CDOM}(440)$ in coastal areas of the ECS is typically lower than 1.0 m^{-1} in most situations, the presence of CDOM does not interfere with this discrimination, even as S_{CDOM} varies from 0.01 to 0.026 nm^{-1}. Despite all of these effects, the discrimination of *P. donghaiense* blooms from diatom blooms based on multispectral measurements of $R_{rs}(\lambda)$ is feasible.

Key words: multispectral reflectance, harmful algal blooms, *Prorocentrum donghaiense*, *Skeletonema costatum*, discrimination

Citation: Tao Bangyi, Pan Delu, Mao Zhihua, Shen Yuzhang, Zhu Qiankun, Chen Jianyu. 2013. Optical detection of *Prorocentrum donghaiense* blooms based on multispectral reflectance. Acta Oceanologica Sinica, 32(10): 48–56, doi: 10.1007/s13131-013-0365-6

1 Introduction

In the Changjiang (Yangtze) River Estuary (CJRE) and the adjacent area of the East China Sea (ECS), a region characterized by typical coastal processes, large-scale dinoflagellate blooms in late spring and early summer have been recorded over the past decade (Li et al., 2009). *Prorocentrum donghaiense* (*P. donghaiense*), which is responsible for marine mammal and fish mortality and is a human health threat, is one of the most common red tide causative dinoflagellates known in this region. The traditional means of identifying harmful algal species requires a direct observation and an enumeration by the light microscopy. Although such methods provide accurate results for algal speciation and relative population abundances, they are time-consuming and labor intensive which limits their use for rapid detection of HABs during bloom conditions when a spatial and temporal variability in the phytoplankton density is present (Sellner et al., 2003). Researchers have shown that algal species may have distinct bio-optical signatures and hence such blooms have the potential to be detected and monitored by some optical approaches (Cullen et al., 1997; Kirkpatrick et al., 2000; Millie et al., 1997; Stæhr and Cullen, 2003).

Over the last decade, an optical remote sensing became an increasingly reliable approach for synoptically detecting and characterizing the location and extent of harmful algal blooms (Cannizzaro et al., 2008; Carvalho et al., 2010; Schofield et al., 1999; Stumpf et al., 2003; Tomlinson et al., 2004). To date, the major tendency in the remote detection of HABs has been the discrimination of toxic algal species using the spectral remote sensing reflectance $R_{rs}(\lambda)$. Several techniques have been developed for the identification of harmful algal blooms associated with specific phytoplankton species from space or airborne ocean color sensors. Most of these techniques use the phytoplankton's spectral signature arising from their inherent optical properties (IOPs), and in particular of the phytoplankton absor-

Foundation item: The National Basic Research Program of China (973 Program) under contract No. 2013CB430302; the National High Technology Research and Development Program of China (863 Program) under contract No. 2007AA092002; the National Natural Science Foundation of China under contract No. 41206170; the public science and technology research funds projects of the ocean under contract No. 201005030; scientific research fund of the Second Institute of Oceanography, SOA under contract No. JG1212.
*Corresponding author, E-mail: pandelu@sio.org.cn

ption coefficient $a_{ph}(\lambda)$. For example, Millie et al. (1997) show that the similarity index (SI), which compares the fourth derivative of $a_{ph}(\lambda)$ of an unknown sample with that of a monospecific *K. brevis* culture, can correctly identify the presence of *K. brevis*. Based on this SI analysis of $a_{ph}(\lambda)$, Craig et al. (2006) explored a hyperspectral approach and developed a method to detect *K. brevis* from $R_{rs}(\lambda)$. In this method, the $a_{ph}(\lambda)$ spectrum was derived from $R_{rs}(\lambda)$ by using a quasi-analytical algorithm (QAA) (Lee and Carder, 2004). However, this approach required hyperspectral instruments with at least 10 nm spectral resolution and high (⩾1 000:1) signal-to-noise ratios (SNR), which are not available in most remote sensing satellites (Kutser et al., 2006).

As multispectral sensors are much more available, it is now more practical to exploit the multispectral patterns of $R_{rs}(\lambda)$ for the detection of specific planktonic species. Shubha et al. (2004) and Westberry et al. (2005) developed semi-analytical models to detect diatoms and the cyanobacterium *Trichodesmium sppz*. Carvalho et al. (2010) introduced a hybrid multispectral algorithm that sequentially applies the optimized versions of an empirical approach and a bio-optical technique for the surveillance of *Karenia brevis*. Many of these optical techniques focus on the direct use of the spectral positions of absorption maxima in a region of 400–500 nm attributable to specific photosynthetic pigments to identify algal groups (Leong and Taguchi, 2006; Millie et al., 1997; Stæhr and Cullen, 2003). However, as the ocean reflectance is determined by the ratio of backscattering to absorption (Gordon et al., 1975) and $R_{rs}(\lambda)$ is inversely proportional to $a(\lambda)$, many spectral features of $a_{ph}(\lambda)$ in the spectral range of 400–500 nm cannot be efficiently characterized by $R_{rs}(\lambda)$, owing to the limitations of noise level of sensors and interference due to the effect of CDOM in the bloom situations. Moreover, most of these studies are primarily dedicated to discrimination of algal blooms associated with specific phytoplankton from normal waters with mixed populations. Only a few algorithms deal with the differentiation of one specific algal bloom from other bloom types. Lubac et al. (2008) demonstrated that the two reflectance ratios [$R_{rs}(490)/R_{rs}(510)$ and $R_{rs}(442.5)/R_{rs}(490)$] can be used to effectively discriminate *P. globosa* blooms from diatom blooms. However, their sensitivity analysis shows that this algorithm, based on two ratios in the blue band, should include information about CDOM concentrations because it interferes with phytoplankton attributed radiometric signals. Generally, the optical discrimination of harmful algal species in coastal waters using the multispectral reflectance remains a challenge, in particular in waters like those in the CJRE and the ECS coastal regions, where suspended sediments and dissolved organic matter of terrestrial origin are present and varying independently.

Despite the effects of other optically significant components, our field measurements have shown that dinoflagellates can be partially discriminated from diatom bloom-forming species based on analyses of their optical properties. The particular spectral signatures in phytoplankton absorption, which are directly related to their pigment composition, are found in the spectral range from 490 to 560 where the values of $a_{ph}(\lambda)$ are relatively low and hence high $R_{rs}(\lambda)$ is observed. Thus, the variations of the spectral shape of $R_{rs}(\lambda)$, caused by differences in the inherent optical properties of these two groups, may provide a potential for their discrimination.

The objective of this study is to explore a multispectral approach for discriminating harmful *P. donghaiense* blooms from diatom blooms. A sensitivity analysis and modeling of a comprehensive reflectance data set for various concentrations and optical parameters are carried out to confirm the potential offered by the characteristics of spectral reflectance in the visible band for identifying the bloom species. This analysis is crucial for providing guidance as to whether this method is likely to work reliably using multispectral ocean color sensors.

2 Materials and method

2.1 *Remote sensing reflectance measurements*

Hyperspectral remote sensing reflectance spectra are derived from above-water measurements of total sea radiance (L_t), sky radiance (L_s), and surface downwelling irradiance (E_s), following NASA ocean optics protocols (Fargion and Mueller, 2001). For each measurement sequence, 15 successive L_t, L_s and E_s spectra were recorded. L_t and L_s were sampled at a relative azimuth angle of 135° away from the sun and at a zenith viewing angle of 40° (Mobley, 1999). E_s spectra were derived by sampling the radiance reflected from a Spectralon plaque with a nominal reflectance of 50%. The measurements were made using an analytical spectral devices 512-channel FieldSpec HandHeld spectrometer that provides high spectral resolution radiometric data with a spectral range of 350–1 050 nm. In the present study, the in situ R_{rs} measurements were made over bloom waters that occurred in the Changjiang River Estuary, the East China Sea from 2006 to 2010.

2.2 *Determination of bio-optical properties of algal*

Simultaneous with the radiometric measurements, a set of subsurface water samples were collected at each station. The measurements of chlorophyll concentration were performed from particulate matter collected on Whatman, GF/F glass fiber filters with a Turner Design TRILOGY fluorometer. Whether the algal community at a particular bloom station was dominated by *P. donghaiens* or diatoms was determined by a microscopic analysis. Note that diatom blooms are almost always dominated by *Skeletonema costatum*.

To accurately derive the bio-optical parameters, such as absorption and scattering properties, isolated cultures of the two phytoplankton species (*P. donghaiense* and the diatom *S. costatum*) were obtained from the Center for Collections of Marine Bacteria and Phytoplankton (CCMBP), at Xiamen University in China. These batch cultures were grown in low light conditions with a 14 h/10 h light/dark cycle at 25°C to match the dominant bloom-forming groups of ECS.

Phytoplankton absorption spectra were determined in an integrating sphere with a central cuvette (CIS) system to avoid errors from scattered light (Nelson and Prézelin, 1993; Röttgers et al., 2007). In this study, the absorption measurements were made with a Perkin-Elmer Lambda 950 spectrophotometer that consists of a Labsphere 150 mm integrating sphere with a centrally mounted sample holder in which a 1-cm-pathlength cuvette was placed. The total absorption for each algal culture in suspension was measured against purified water as reference. The absorption of 0.22 μm filtrate of the culture medium was determined in the same way, and subtracted from the total absorption of the algal culture (Röttgers et al., 2007; Yentsch, 1962). The spectral absorption coefficients for different substances were calculated from the optical density $OD(\lambda)$ as the following:

$$a(\lambda) = 2.303[OD_s(\lambda) - OD_f(\lambda)]/0.01. \quad (1)$$

In addition, the scattering coefficients, $b(\lambda)$, was indirect-

ly obtained from successive measurements of absorption $a(\lambda)$ and attenuation $c(\lambda)$ according to the principle $c(\lambda) = a(\lambda) + b(\lambda)$. Nominally, the attenuation coefficients can also be obtained by measuring beam transmittance with a spectrophotometer. To minimize the error of $c(\lambda)$ due to forward scattered light seen by the detector, the attenuation measurements were made with a Perkin-Elmer Lambda 35 spectrophotometer by placing the sample cuvette close to the output window of the sample beam, and the half-angle was reduced to about 0.23° by using an additional custom cuvette with an aperture of 0.8 mm in front of the detector. While $c(\lambda)$ is still slightly underestimated, the error of $c(\lambda)$ has been estimated to be considerably lower than 5% (Bricaud and Morel, 1986). The calculation of $c(\lambda)$ for different substances was as the same as that of the $a(\lambda)$.

To avoid errors from multiple scattering within the cuvette, the suspension samples were serially diluted and the measurements of absorption and attenuation were made at decreasing concentrations. Only those measurements in which a linear relationship between measured value and the dilution factor was established were utilized.

2.3 *Radiative transfer modeling*

To identify *P. donghaiense* blooms with multispectral remote sensors, we will use two ratios of $R_{rs}(\lambda)$ taken in the visible part of the spectrum. We hypothesized that other optically significant components, except for phytoplankton, have an effect on the efficacy of the two ratios. Therefore a sensitivity analysis was conducted to evaluate their impact. Specifically, we tested the effects of variable chlorophyll concentration, CDOM, and the composition of the particulates (through the backscattering ratio, b_{bp}/b_p). The HYDROLIGHT radiative transfer model, which computes the radiance distribution in the ocean, was employed to conduct the sensitivity analysis.

A three-component model, which consists of seawater, CDOM, and algal particles, was used to calculate the optical properties of variable bloom waters with different values of chlorophyll concentration, CDOM concentration and backscattering fraction b_{bp}/b_p. Thus, the scattering and absorption spectra are represented as follows:

$$a(\lambda) = a_w(\lambda) + a_{ph}(\lambda) + a_{CDOM}(\lambda), \quad (2)$$

$$b(\lambda) = b_w(\lambda) + b_{ph}(\lambda), \quad (3)$$

where $a_w(\lambda)$ and $b_w(\lambda)$ are the pure seawater absorption and scattering coefficients, values of which were taken from the results of Pope and Fry (1997), $b_{ph}(\lambda)$ is the phytoplankton scattering coefficient, and $a_{ph}(\lambda)$ and $a_{CDOM}(\lambda)$ are the phytoplankton and colored dissolved organic matter absorption coefficients, respectively. In addition, the absorption of the nonalgal particles $a_{nap}(\lambda)$ has a spectral shape similar to $a_{CDOM}(\lambda)$, and during our investigated algal bloom waters, the nonalgal particles only account for less than 5% of the total absorption, even in the blue bands. Therefore $a_{nap}(\lambda)$ is not included in the model. The phytoplankton spectra of $a_{ph}(\lambda)$ and $b_{ph}(\lambda)$ were considered proportional to chlorophyll concentration (c_{Chl}) and then parameterized as:

$$\left.\begin{aligned} a_{ph}(\lambda) &= c_{Chl} a^*_{ph}(\lambda), \\ b_{ph}(\lambda) &= c_{Chl} b^*_{ph}(\lambda), \end{aligned}\right\} \quad (4)$$

where $a^*_{ph}(\lambda)$ and $b^*_{ph}(\lambda)$ were specific absorption and scattering coefficients of each algal culture, values of which were obtained from laboratory measurements made on both monospecific cultures of *P. donghaiense* and *S. costatum*. The absorption by CDOM was modeled from the expression:

$$a_{CDOM}(\lambda) = a_{CDOM}(\lambda_0) \times \exp\left[-S_{CDOM}(\lambda - \lambda_0)\right], \quad (5)$$

where $\lambda_0 = 440$ nm and S_{CDOM} is the spectral slope. Furthermore, the scattering phase function (SPF) of sea water, $P(\phi)$, is crucial for determining remote-sensing reflectance. In addition to pure-water SPF $P_w(\phi)$, that have been well studied, HYDROLIGHT required the backscattering ratio of particle b_{bp}/b_p to derive SPFs of algal particles $P_{ph}(\phi)$ (Fournier and Forand, 1994; Mobley et al., 2002). The spectral dependence of the particulate backscattering ratio was found to not be significant (4%–10% variability between wavelengths) (Whitmire et al., 2007). Therefore, the b_{bp}/b_p ratio was taken to be constant over the entire spectral range and user defined (see below).

HYDOLIGHT simulations were performed in the VIS and NIR spectral range from 400 nm to 800 nm. It was assumed that the IOPs were uniformly distributed throughout the water column and the water column was deep enough to avoid any bottom effects. Since light attenuates very rapidly with depth in bloom waters, these assumptions were considered to be reasonable. Moreover, the simulations were performed for a clear sky with the sun at the zenith and a nominal wind speed of 5 m/s (to simulate surface roughening) and the surface irradiance was calculated using the RADTRAN model supplied as part of the HYDROLIGHT code.

Four HYDROLIGHT scenarios were modeled. For each scenario except Scenario I, chlorophyll concentration successively takes a value of 5, 10, 30, 50 and 100 mg/m^3 for the two examined algal species. In Scenario I, b_{bp}/b_p, $a_{CDOM}(440)$ and S_{CDOM} were held constant at 0.01, 0.1 m^{-1} and 0.014 nm^{-1}, respectively, while the chlorophyll concentration was allowed to vary from 2 to 100 mg/m^3. In Scenario II, $a_{CDOM}(440)$ and S_{CDOM} were held constant at 0.1 m^{-1} and 0.014 nm^{-1}, respectively, while b_{bp}/b_p was allowed to vary from 0.003 to 0.030. This range of b_{bp}/b_p values encompasses both the realistic range and extreme values. In Scenario III, b_{bp}/b_p, and S_{CDOM} were held constant at 0.01, and 0.014 nm^{-1}, respectively, while $a_{CDOM}(440)$ was varied from 0.0 to 1.5 m^{-1}. This range of $a_{CDOM}(440)$ exceeds the realistic range observed in the coastal area of the ECS. In Scenario IV, b_{bp}/b_p, was held constant at 0.01 and $a_{CDOM}(440)$ was set to either 1.5 or 1.0 m^{-1}, while S_{CDOM} was increased from 0.010 to 0.026 nm^{-1}. This range S_{CDOM} is within the range of values observed in situ.

3 Results and discussion

3.1 *Comparative optical properties of algal species*

To address the utility of using $R_{rs}(\lambda)$ for detecting and discriminating harmful algal blooms, IOPs of the phytoplankton need to be analyzed, especially the difference in the absorption properties of the two examined phytoplankton species is most responsible for spectral behaviors of $R_{rs}(\lambda)$ (Mao et al., 2010). Figures 1a and 1b show the normalized absorption and scattering spectra for *P. donghaiense* and the diatom *S. costatum* measured from the laboratory cultures. To facilitate comparison, the phytoplankton absorption and scattering spectra were normalized to their mean value of 400 to 700 nm. *P. donghaiense* is a peridinin-containing dinoflagellate, while the diatom *S. costatum* has the characteristic pigment fucoxanthin. Both of these pigments have a significant impact on the green wavelength range of the phytoplankton absorption spectrum (Bricaud et al., 2004), although the specific absorption coeffi-

cients of their component pigments have not been uniformly determined (Bidigare et al., 1990; Hoepffner and Sathyendranath, 1991; Majchrowski and Osthowska, 2000). The spectral shapes of the two absorption spectra differ mainly in the 490–560 nm spectral domain where *P. donghaiense* shows a much stronger negative spectral slope than that of *S. costatum*. Furthermore, in the same spectral domain, while the slope of the scattering spectrum of *S. costatum* is very close to 0, the slope of the specific scattering spectra for *P. donghaiense* is positive (Fig.1b). These characteristics may directly impact on the remote sensing reflectance owing to its direct relation to the single scattering albedo (ω_0) that is calculated from the absorption and scattering coefficients.

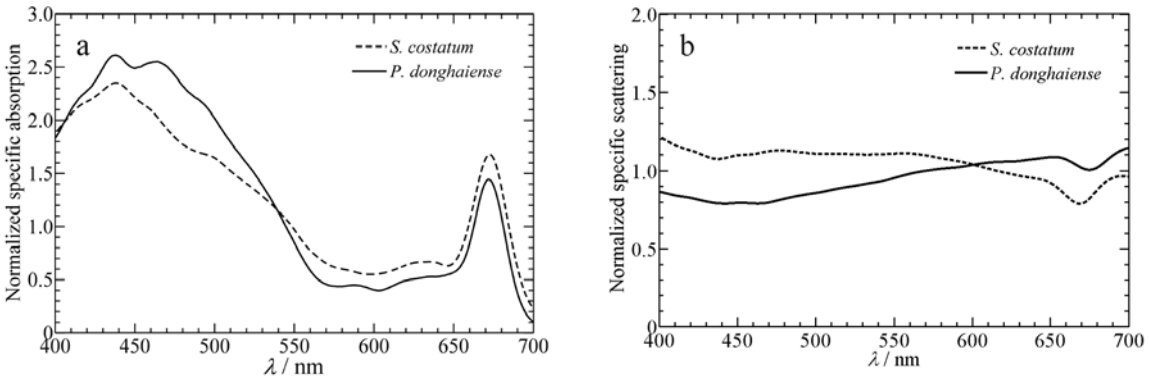

Fig.1. Normalized absorption (a) and scattering (b) spectra of *P. donghaiense* and the diatom *S. costatum* obtained from cultures. The normalization is performed using the mean value of each spectrum from 400 to 700 nm.

The in situ $R_{rs}(\lambda)$ data set of algal bloom waters was collected in the coastal areas of the ESC which includes the two phytoplankton taxonomic groups; the dinoflagellate *P. donghaiense* and the diatom *S. costatum*. The selected $R_{rs}(\lambda)$ spectra with chlorophyll concentration greater than 4.0 mg/m^3 are shown in Fig.2. The $R_{rs}(\lambda)$ spectra associated with *S. costatum* were taken for chlorophyll concentration ranging from near 4.4 to 41.2 mg/m^3, while the ones associated *P. donghaiense* had chlorophyll concentration spanning from 14.2 to 112 mg/m^3. As is seen, the $R_{rs}(\lambda)$ spectra vary significantly over the visible and NIR spectral regions, yet these spectra are typical of a phytoplankton bloom situation with minimal values in the blue region (400–500 nm) and two peaks near 560 nm and 700 nm. The dramatic difference between the two $R_{rs}(\lambda)$ groups is the wider range of depression between 400 and 530 nm without defined spectral features for *P. donghaiense*, where several MERIS and MODIS bands (shading) are located. To characterize the features of this depressed R_{rs} region, we compare the R_{rs} spectra for *P. donghaiense* and *S. costatum* with high, but similar, chlorophyll concentration of 42.5 mg/m^3 and 41.2 mg/m^3, respectively. The two selected spectra (red curves in Fig. 2) were normalized by the maximum value of each spectrum near 575 nm, and are shown in Fig.3a. For such high chlorophyll concentration, this lack of reflectance feature continues into the green range as far as 540 nm and hence results in the sharper increase of normalized $R_{rs}(\lambda)$ $[nR_{rs}(\lambda)]$ of *P. donghaiense* in the spectral range from 530 to 560 nm, which corresponds to a strong decrease in the $a_{ph}(\lambda)$ spectra in this region. The first derivatives of the two $nR_{rs}(\lambda)$ $\{d[nR_{rs}(\lambda)]/d\lambda\}$ spectra were also calculated and are shown in Fig.3b. The most distinguishing feature is the peak in the first derivative near 560 nm. The peak of *P. donghaiense* is almost twice the value of *S. costatum*.

As a maximum in the $a(\lambda)$ spectrum corresponds to a minimum in the $R_{rs}(\lambda)$ spectrum, many spectral features of $a_{ph}(\lambda)$ in the spectral range of 400–500 nm cannot be efficiently observed in the spectrum of $R_{rs}(\lambda)$ in the bloom waters. In addi-

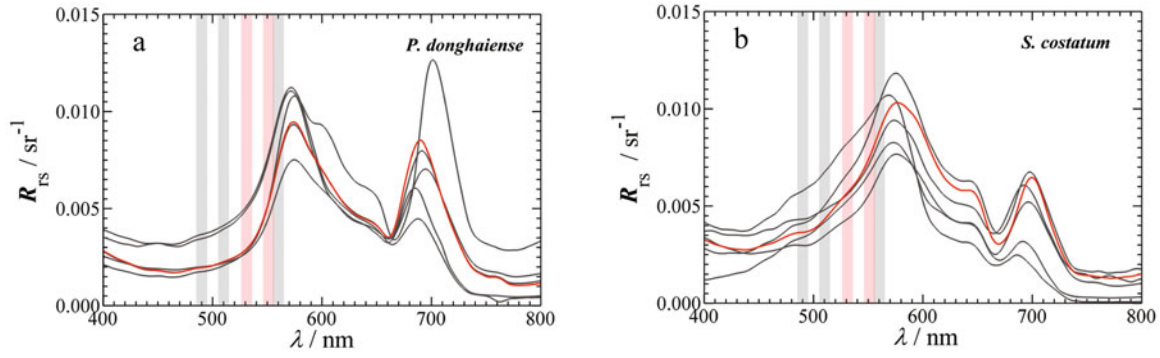

Fig.2. Hyperspectral $R_{rs}(\lambda)$ spectra of the algal bloom waters, which were obtained from field measurements performed in the Changjiang (Yangtze) River Estuary and the coastal area of the East China Sea. The following two examples are highlighted in red: a. *P. donghaiense*, c_{Chl}=42.5 mg/m^3 and b. *S. costatum*, c_{Chl}=41.2 mg/m^3. The positions and widths of spectral bands in the MERIS and MODIS baseline band-set are plotted as gray and red vertical bars.

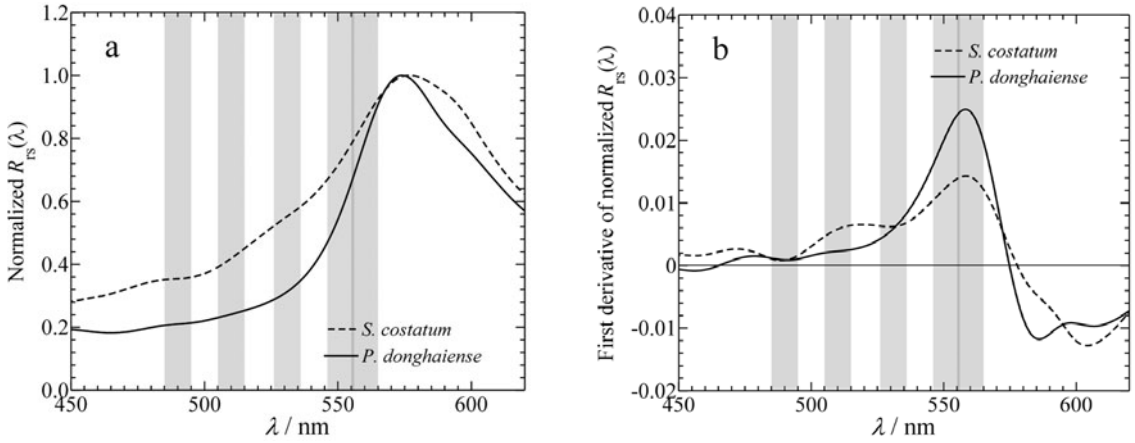

Fig.3. Normalized spectra of two highlighted $R_{rs}(\lambda)$ in Fig.2 associated with *P. donghaiense* and the diatom *S.costatum*, respectively (a); and their first derivatives. The normalization is performed using the maximum value of each spectrum in the green region (b).

tion, for turbid waters, with chlorophyll concentration greater than 5.0 mg/m^3, the spectral dependence of $b_{bp}(\lambda)$ in phytoplankton cultures is not significant in comparison with $a_{ph}(\lambda)$ (Loisel et al., 2006; Whitmire et al., 2010). Consequently, b_b of the two bands can be assumed almost equal when the two wavelengths are very close to each other, especially in the spectral range where the pigment absorption is not significant. Therefore, if the difference value of the absorption between the two bands is constant, then the percent difference of $R_{rs}(\lambda)$ between the two bands is inversely proportional to mean value of their $a_{ph}(\lambda)$. These facts indicate that, owing to the spectral decrease of $a_{ph}(\lambda)$ in the range of 490 to 560 nm, the $R_{rs}(\lambda)$ in the range of 510 to 560 have two advantages for the discrimination of harmful algal blooms; relative high reflectance during bloom conditions and high sensitivity to the variability in the $a_{ph}(\lambda)$. Therefore, the spectral variability of first derivatives of $nR_{rs}(\lambda)$ near 560 nm, $d\lambda nR_{rs}(560)$, is in agreement with the analysis presented above, and is sufficiently high for the discrimination of *P. donghaiense* blooms from diatom blooms.

3.2 *Species differentiation by two ratios*

The intent of this paper is to explore a multispectral approach for the remote discrimination of *P. donghaiense*. Thus, we try to examine the utility of using multispectral $R_{rs}(\lambda)$ to define the spectral feature of the $R_{rs}(\lambda)$. In this study, $d\lambda nR_{rs}(\lambda)$ is estimated using a finite difference approximation:

$$\frac{dnR_{rs}(\lambda_2)}{d\lambda} \backsimeq \frac{R_{rs}(\lambda_2)-R_{rs}(\lambda_1)}{(\lambda_2-\lambda_1)} \Big/ R_{rs}\left(\lambda_{mg}\right), \quad (6)$$

where λ_{mg} is wavelength of maximum reflectance in the green spectral range. Based on our in situ observations presented above, in bloom situations the max $R_{rs}(\lambda)$ in the green band close to 560 nm and the major difference in $d\lambda nR_{rs}(\lambda)$ of the two examined algal species occur near 560 nm. Therefore as a first approximation, we assumed that λ_{mg} for both species are equal to λ_2. As the band deviation $(\lambda_2-\lambda_1)$ is identical during the calculation, we finally assumed that the $d\lambda nR_{rs}(\lambda_2)$ was directly proportional to the band ratio $[R_{rs}(\lambda_2)/R_{rs}(\lambda_1)]$.

$$\frac{dnR_{rs}(\lambda_2)}{d\lambda} \propto \frac{R_{rs}(\lambda_2)}{R_{rs}(\lambda_1)}. \quad (7)$$

Thus in the following discrimination, we will use the ratio with bands near 560 nm (denoted as R_1) to characterize the spectral feature near 560 nm.

The spectral ratio derived in the algal bloom waters will show a significant relationship with chlorophyll concentration or the biomass of phytoplankton (Gordon and Morel, 1983; O'Reilly et al., 1998). For practical application, indicies also derived from $R_{rs}(\lambda)$ should be taken to characterize algal populations dominated by *P. donghaiense* and the diatom *S. costatum*. Recently, Gilerson et al. (2010) found that two-band algorithms with bands in the red-NIR spectral range are more effective than blue-to-green ratio algorithms for the estimation of chlorophyll concentrations in turbid waters. Thus the two-band ratios with MODIS bands $R_{rs}(748)/R_{rs}(667)$ or MERIS bands $R_{rs}(708)/R_{rs}(665)$ (denoted as R_2) are currently used as indices for chlorophyll.

With a combination of R_1 and R_2 band ratios, a two-ratio model is developed for the identification of phytoplankton groups. To evaluate potential of current multispectral ocean color sensors for the discrimination of dominant bloom species, we have tested all possible combinations between the R_1 ratio for the band set of MERIS and MODIS [443, 490, 510 nm (MERIS), 532, 555 nm (MODIS), and 560 nm (MERIS)] and the R_2 ratio applied to in situ R_{rs} data in Fig. 2. The selected results are shown in Fig. 4. For illustrative purposes, the least squares linear fit is performed on each data group. More accurate fits that are in accord with the natural behavior of the two ratios will be discussed in the next section. The three panels on the top row of Fig. 4 represent the results tested with the MODIS bands, for which the R_1 calculation used λ_2=555 nm and λ_1 increases from the left to the right (λ_1=443, 490 or 532 nm). As seen, when λ_1=443 nm, the results associated with *P. donghaiense* are not separated from those associated with *S. costatum*. This could be due to interference from the variation in the concentration of other optically significant components such as CDOM. When λ_1=490 nm, although results are beginning to separate, the interference still remains significant. By λ_1=532 nm, the discrimination shows better performance as *P. donghaiense* blooms can be effectively separated by their R_1 value. Similarly, MERIS bands are also tested (Figs 4d–e) with λ_2=560 nm and λ_1=490 or 510 nm for the R_1 calculation. In comparison with the MODIS, the R_1 ratio using the MERIS bands is more effective for the discrimination, which can be primarily attributed to the fact the MERIS band is centered at 560 nm. Since the

band centered at 510 nm is still a little too far from 560 nm, the R_1 ratio is also tested for the MERIS 560 nm and the MODIS 532 nm bands. As seen in Fig. 4f, the relationship between the R_1 [$R_{rs}(560)/R_{rs}(532)$] of *S. costatum* and the R_2 [$R_{rs}(708)/R_{rs}(665)$] ratio behaves in a more regular way than that in other panels of Fig. 4. Consequently, the *P. donghaiense* and *S. costatum* blooms can be best discriminated by using this R_1 ratio. This is because that the two-band MODIS model $R_{rs}(748)/R_{rs}(667)$ has been proven to be less accurate than the two-band MERIS model which is due to the higher uncertainty in retrieved reflectance at 748 nm and some inaccurate assumptions about backscattering coefficients (Gilerson et al., 2010; Moses et al., 2009). Most importantly, the two bands at 530 and 560 nm are close enough to accurately define the slope near 560 nm. Thus, the best combination of R_1 and R_2 has been found between the $R_{rs}(560)$ to $R_{rs}(532)$ for the ratio (R_1) and the $R_{rs}(708)$ to $R_{rs}(665)$ for the ratio (R_2).

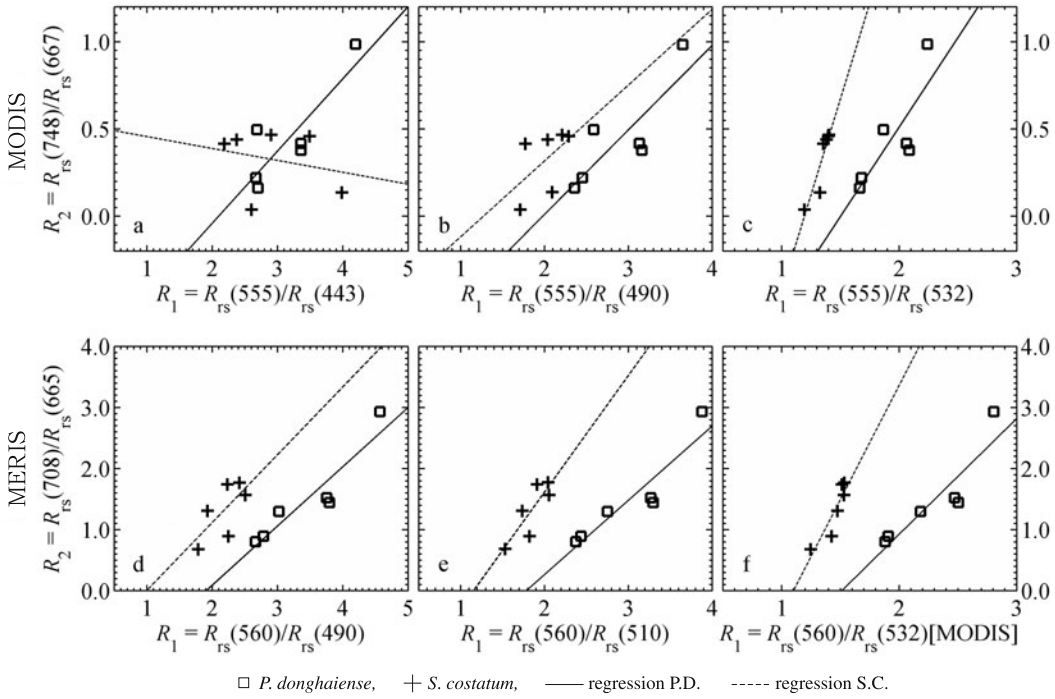

Fig.4. Variation of R_1 as a function of R_2 for various combinations of R_{rs} ratios from the set of MODIS and MERIS bands. The bloom stations associated with chlorophyll concentration levels higher than 5.0 mg/m^3 are selected. The blooms identified as dominated by *P. donghaiense* and *S. costatum* are represented by blue circles and black triangles, respectively. The curves obtained by linear least squares fit for *P. donghaiense* and *S. costatum* are represented by solid and dash lines, respectively (P.D is abbreviated from *Prorocentrum donghaiense*, and S.C *Skeletonnema costatum*).

3.3 *Sensitivity analysis*

Given these encouraging results, it is necessary to assess whether this pattern is really due to the differences in the spectral optical properties of the two phytoplankton species and to evaluate the sensitivity of each ratio to variations in other bio-optical parameters. Thus, four computational scenarios, in which chlorophyll concentration, b_{bp}/b_p, $a_{CDOM}(440)$ and S_{CDOM} vary independently, are examined. For convenience, we use modeled ratios from the band centers of the synthetic data, $R_{rs}(\lambda)$ instead of the integrating one, for the latter does not produce a noticeable change in the band ratios.

Figure 5a (Scenario I) shows that, as the total chlorophyll concentration increases, both R_1 and R_2 increase for both species. For extremely low chlorophyll concentration (i.e., low biomass), the R_2 ratio tends toward a limit which is imposed by the optical properties of pure water; conversely, at very high chlorophyll concentration, the R_1 ratio is governed by the optical properties of phytoplankton cells and also tends toward a limit. The existence of these two limiting value imposes a power law to the curve representing the relationship between R_1 and R_2. An empirical relationship accounts for this curvature and creates the power law relationship, instead of a linear one in Fig. 5b. This relationship was redrawn from in situ data sets in Fig. 4f with the inclusion of the result from a bloom station dominated by the dinoflagellate at a chlorophyll concentration of 2.3 mg/m^3. The analysis of both the measurements and the synthetic data reveal that R_1 is more sensitive to the variation of chlorophyll concentration than R_2 when chlorophyll concentration increases from low to moderate, but then becomes less sensitive at high chlorophyll concentration. For chlorophyll concentration less than 5 mg/m^3, the two phytoplankton groups cannot be separated from either R_1 or R_2 because the biomass is too low. When the chlorophyll concentration increases to 10 mg/m^3, the R_1 ratio begins to discriminate the two groups. When the chlorophyll concentration exceeds 20 mg/m^3, R_2 values for both *P. donghaiense* and *S. costatum* blooms are near 1.0. Further increasing chlorophyll causes the R_1 values for *P. donghaiense* to asymptote to a limiting value of 2.7, while the one of *S. costatum* asymptotes to a lower limiting value of 1.7. Thus, we define two criteria necessary to discriminate the *P. donghaiense* blooms from diatom blooms: the value of R_1 [$R_{rs}(560)/R_{rs}(532)$] has to be observed beyond 1.55 when

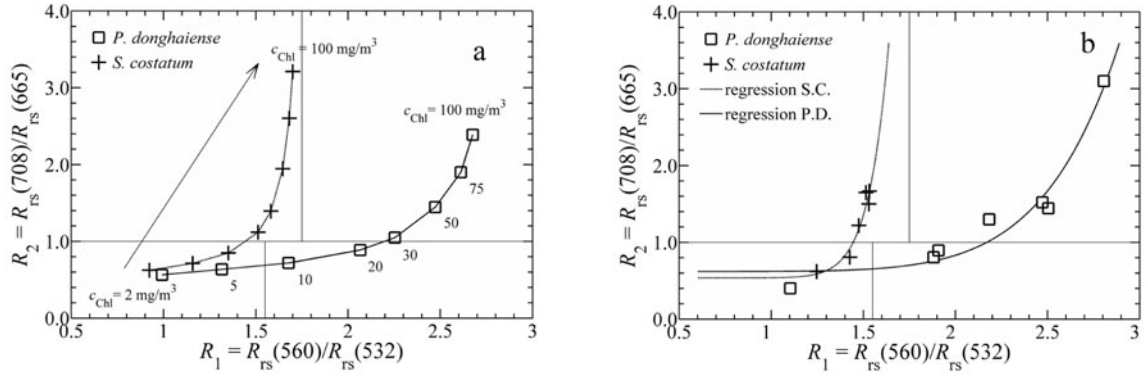

Fig.5. Scenario I: variation of R_1 as a function of R_2 from numerical simulations performed for the analysis of sensitivity to varying chlorophyll concentrations, when $a_{CDOM}(440)$ and b_{bp}/b_p are held constant and the chlorophyll concentration vary from 2 to 100 mg/m^3 (a); and as in Fig.4f except for that a bloom station associated with a chlorophyll concentration of 2.3 mg/m^3 and dominated by the dinoflagellate is included, and that curves of power fit take the place of those of linear fit (b).

R_2 [$R_{rs}(708)/R_{rs}(665)$] is smaller than 1.0, and the value of R1 has to be observed beyond 1.75 when R_2 is higher than 1.0, as plotted in Fig. 5a.

For each c_{Chl}, as the b_{bp}/b_p decreases from 0.003 to 0.030 while $a_{CDOM}(440)$ and S_{CDOM} are held constant (Scenario II), R_1 and R_2 increase (Fig. 6). As in Scenario I, *P. donghaiense* and *S. costatum* are very well discriminated in the (R_1, R_2) phase space. Although R_1 is more sensitive to the variation of b_{bp}/b_p than R_2, for chlorophyll concentration values greater than 10 mg/m^3, the minimum difference between the R_1 values calculated for the two phytoplankton communities is found to be greater than 0.4 when R_2 <1.0 and 0.8 when R_2 >1.0. Consequently, the two criteria defined above can easily separate the *P. donghaiense* blooms from *S. costatum* ones even when b_{bp}/b_p varies by such a large extent.

However, because its absorption at the short wavelength may dominate the phytoplankton absorption, CDOM may be the main optically significant component that has the potential to cause significant impact on the R_1 ratio in an algal bloom situation. Figure 7 shows the result of the sensitivity analysis of the effect of variation in the concentration of CDOM. With b_{bp}/b_p held constant, the $a_{CDOM}(440)$ varies from 0 to 1.5 m^{-1} while the chlorophyll concentration increases from 5 to 100 mg/m^3 (Scenario III). It is clear that the R_1 ratio of *P. donghaiense* is more sensitive to the CDOM concentrations than that of *S. costatum*, while the R_2 ratio shows very little variation. It is probable that there is also a dependence of R_1 on the spectral slope of CDOM when the absorption due to CDOM is comparable to that due to the phytoplankton. In Scenario IV, the influence of S_{CDOM} is investigated. Figure 8 shows the dependence of R_1 and R_2 on S_{CDOM} at two selected CDOM concentrations. There is a positive relationship between the magnitude of R_1 ratio and S_{CDOM}. Decreasing S_{CDOM} below 0.026 nm^{-1} is seen to decrease the R_1 value of a *P. donghaiense* bloom to outside of the two defined criteria, and conversely, increasing S_{CDOM} above 0.014 nm^{-1} is seen to increase of R_1 of *S. costatum* into these criteria, because the slope of $a_{CDOM}(\lambda)$ can either enhance or reduce slopes of the total absorption spectra. When $a_{CDOM}(440)$=1.0 m^{-1}, the reflectance curves are less effected by the presence of CDOM,

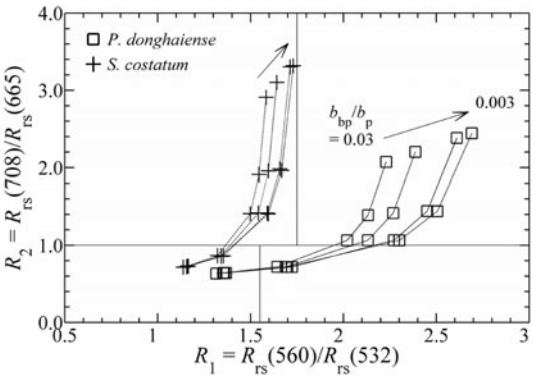

Fig.6. Scenario II sensitivity analysis of the b_{bp}/b_p effect: the b_{bp}/b_p vary from 0.003 to 0.030, when $a_{CDOM}(440)$ is held constant and the chlorophyll concentration increases from 5 to 100 mg/m^3.

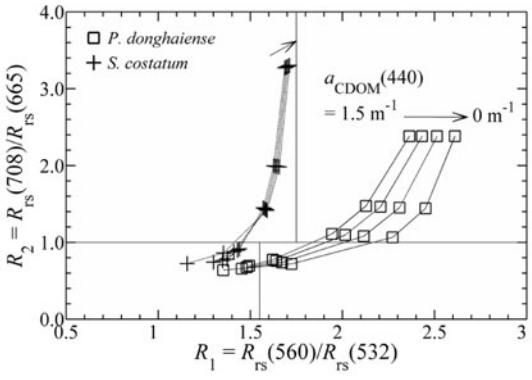

Fig.7. Scenario III sensitivity analysis of the effect of CDOM concentrations: the $a_{CDOM}(440)$ vary from 0 to 1.5 m^{-1}, when S_{CDOM} and b_{bp}/b_p are held constant of 0.014 nm^{-1} and 0.01 and the chlorophyll concentration increases from 5 to 100 mg/m^3.

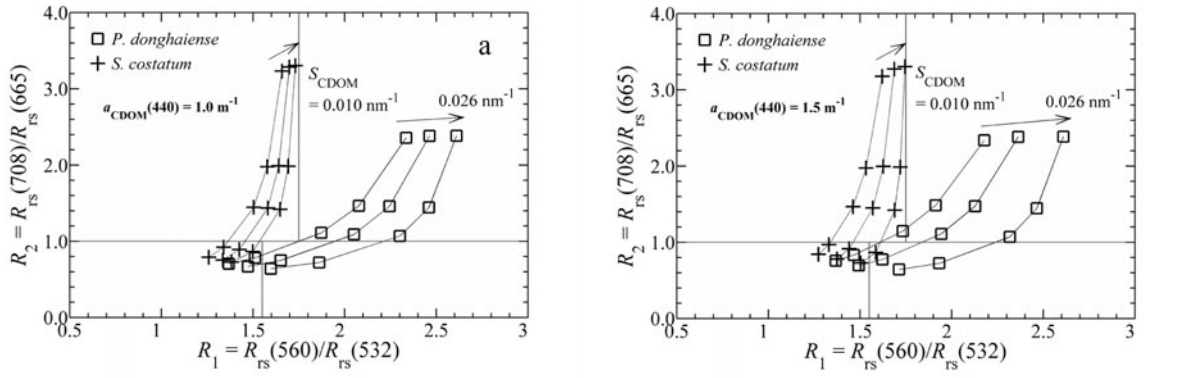

Fig.8. Scenario IV sensitivity analysis of the CDOM slope (S_{CDOM}) effect: the S_{CDOM} vary from 0.010 to 0.026 nm^{-1}, when b_{bp}/b_p is held constant and chlorophyll concentration increases from 5 to 100 mg/m^3. $a_{CDOM}(440)$=1.0 m^{-1} (a); and $a_{CDOM}(440)$=1.5 m^{-1} (b).

so that the two criteria defined for the discrimination are still suitable. Only under the extreme conditions, when S_{CDOM}=0.026 nm^{-1} and $a_{CDOM}(440)$>1.5 m^{-1} is the presence of CDOM possibly problematic for this discrimination. Fortunately, in the coastal areas of the ECS, the maximum value of $a_{CDOM}(440)$ does not exceed 0.5 m^{-1} even in summer when CDOM dominates the total seawater absorption (Hui et al., 2012), and in an algal bloom, with chlorophyll concentration as high as 112 mg/m^3, our in situ measurements of $a_{CDOM}(440)$ only approach 0.45 m^{-1}.

4 Conclusions

In this paper, we explored a multispectral approach to discriminate dinoflagellate *P. donghaiense* dominated blooms from diatom *S. costatum* dominated blooms by the in situ R_{rs} measurements. A distinct spectral pattern of $a_{ph}(\lambda)$ is found in measurements from cultures, wherein the specific absorption of *P. donghaiense* decreases much more sharply than that of *S. costatum* in the range from 490 to 560 nm. This feature gives rise to an optical signature in R_{rs} and hence the first derivatives of R_{rs} near 560 nm that are sufficiently unique to allow their use to define a set of identification criteria to distinguish between *P. donghaiense* and *S. costatum* dominated blooms.

To evaluate the potential of current multispectral ocean color sensors for use in the discrimination, a two-band ratio (denoted as R_1) is taken to characterize the spectral feature near 560 nm. Because of sensitivity to chlorophyll concentration, another two-band ratio in the red-NIR range is employed as an index for chlorophyll concentration level. Based on these two ratios, a model is developed for the differentiation of *P. donghaiense* and *S. costatum* dominated blooms. We test all possible combinations of the R_1 ratio near 560 nm and R_2 ratio from the set of MERIS and MODIS bands. The best combination found to identify blooms of *P. donghaiense* is following the two reflectance ratios: $R_{rs}(560)/R_{rs}(532)$ (R_1) and $R_{rs}(708)/R_{rs}(665)$ (R_2).

To investigate the effects of varying levels of chlorophyll concentration, CDOM, and backscattering ratio (b_{bp}/b_p) on the efficacy of this multispectral approach, we undertook a combination of a three-component, bio-optical model and the HYDROLIGHT radiative transfer code to simulate four water column scenarios for the various sensitivity analysis. Scenario I simulations reveal that the composition and the intensity (i.e., the chlorophyll concentration value) of the algal blooms can explain much of the behavior of R_1 versus R_2 in situ (Fig. 5b). Two criteria ($R_1 > 1.55$ when $R_2 < 1.0$ and $R_1 > 1.75$ when $R_2 \geqslant 1.0$) are established for this discrimination based upon the analysis of both the measurement and synthetic data. Scenario II simulations show that, although both R_1 and R_2 are sensitive to the variation in the b_{bp}/b_p, the discrimination between *P. donghaiense* and *S. costatum* blooms is not significantly affected by the nature of the bulk particulates as the b_{bp}/b_p value. Scenario III and IV simulations indicate that only under the extreme conditions, such as $a_{CDOM}(440)$>1.5 m^{-1}, which do not naturally occur in the coast areas of the ECS, would the presence of CDOM be problematic for this discrimination. When $a_{CDOM}(440)$ is lower than 1.0 m^{-1}, the defined two criteria are still suitable for the discrimination and are less effected by the presence of CDOM, even as S_{CDOM} varies from 0.010 to 0.026 nm^{-1}.

These results suggest that the regional-scale discrimination of *P. donghaiense* blooms based on multispectral measurements of $R_{rs}(\lambda)$ may be feasible. As our results are based on in situ measurements of R_{rs}, this multispectral approach should be initially used to complement and enhance current real-time in situ monitoring of algal blooms, as well as practically applied to satellite measurements of R_{rs}, which should be included in future work.

References

Bidigare R R, Ondrusek M E, Morrow J H, et al. 1990. In vivo absorption properties of algal pigments. Proc SPIE 1302, Ocean Optics X, 290–302

Bricaud A, Claustre H, Ras J, et al. 2004. Natural variability of phytoplanktonic absorption in oceanic waters: influence of the size structure of algal populations. Journal of Geophysical Research, 109: C11010

Bricaud A, Morel A. 1986. Light attenuation and scattering by phytoplanktonic cells: a theoretical modeling. Applied Optics, 25(4): 571–580

Cannizzaro J P, Carder K L, Chen F R, et al. 2008. A novel technique for detection of the toxic dinoflagellate, *Karenia brevis*, in the Gulf of Mexico from remotely sensed ocean color data. Continental Shelf Research, 28(1): 137–158

Carvalho G A, Minnett P J, Fleming L E, et al. 2010. Satellite remote sensing of harmful algal blooms: a new multi-algorithm method for detecting the Florida red tide (*Karenia brevis*). Harmful Algae, 9(5): 440–448

Craig S E, Lohrenz S E, Lee Z, et al. 2006. Use of hyperspectral remote sensing reflectance for detection and assessment of the harmful alga, *Karenia brevis*. Applied Optics, 45(21): 5414–5425

Cullen J J, Ciotti á M, Davis R F, et al. 1997. Optical detection and assessment of algal blooms. Limnology and Oceanography, 42(5 II): 1223–1239

Fargion G S, Mueller J L, 2001. Ocean optics protocols for satellite ocean color sensor validation, Revision 3 (NASA technical memorandum). National Aeronautics and Space Administration, Goddard Space Flight Center, Maryland

Fournier G R, Forand J L. 1994. Analytic phase function for ocean water. Ocean Optics XII. SPIE. Bergen, Norway

Gilerson A A, Gitelson A A, Zhou J, et al. 2010. Algorithms for remote estimation of chlorophyll-a in coastal and inland waters using red and near infrared bands. Optics Express, 18(23): 24109–24125

Gordon H R, Brown O B, Jacobs M M. 1975. Computed relationships between the inherent and apparent optical properties of a flat homogeneous ocean. Applied Optics, 14(2): 417–427

Gordon H R, Morel A Y. 1983. Remote assessment of ocean color for interpretation of satellite visible imagery: a review. In: Barber T R, Mooers C N K, Bowman M J, et al., eds. Lecture Notes on Coastal and Estuarine Study. New York: Springer-Verlag, 1–114

Hoepffner N, Sathyendranath S. 1991. Effect of pigment composition on absorption properties of phytoplankton. Mar Ecol Prog Ser, 73: 11–23

Lei Hui, Pan Delu, Bai Yan, et al. 2012. The proportions and variations of the light absorption coefficients of major ocean color components in the East China Sea. Acta Oceanologica Sinica, 31(2): 45–61

Kirkpatrick G J, Millie D F, Moline M A, et al. 2000. Optical discrimination of a phytoplankton species in natural mixed populations. Limnology and Oceanography, 45(2): 467–471

Kutser T, Metsamaa L, Strömbeck N, et al. 2006. Monitoring cyanobacterial blooms by satellite remote sensing. Estuarine, Coastal and Shelf Science, 67(1–2): 303–312

Lee Z, Carder K L. 2004. Absorption spectrum of phytoplankton pigments derived from hyperspectral remote-sensing reflectance. Remote Sensing of Environment, 89(3): 361–368

Leong S, Taguchi S. 2006. Detecting the bloom-forming dinoflagellate *Alexandrium tamarense* using the absorption signature. Hydrobiologia, 568(1): 299–308

Li J, Glibert P M, Zhou M, et al. 2009. Relationships between nitrogen and phosphorus forms and ratios and the development of dinoflagellate blooms in the East China Sea. Mar Ecol Prog Ser, 383: 11–26

Loisel H, Nicolas J M, Sciandra A, et al. 2006. Spectral dependency of optical backscattering by marine particles from satellite remote sensing of the global ocean. Journal of Geophysical Research: Oceans, 111(C9): C09024

Lubac B, Loisel H, Guiselin N, et al. 2008. Hyperspectral and multispectral ocean color inversions to detect *Phaeocystis globosa* blooms in coastal waters. Journal of Geophysical Research, 113(C6): C06026

Majchrowski R, Osthowska M. 2000. Influence of photo- and chromatic acclimation on pigment composition in the sea. Oceanologia, 42(2): 157–175

Mao Z, Stuart V, Pan D, et al. 2010. Effects of phytoplankton species composition on absorption spectra and modeled hyperspectral reflectance. Ecological Informatics, 5(5): 359–366

Millie D F, Schofield O M, Kirkpatrick G J, et al. 1997. Detection of harmful algal blooms using photopigments and absorption signatures: A case study of the Florida red tide dinoflagellate, *Gymnodinium breve*. Limnology and Oceanography, 42(5): 1240–1251

Mobley C D. 1999. Estimation of the remote-sensing reflectance from above-surface measurements. Applied Optics, 38(36): 7442–7455

Mobley C D, Sundman L K, Boss E. 2002. Phase function effects on oceanic light fields. Applied Optics, 41(6): 1035–1050

Moses W J, Gitelson A A, Berdnikov S, et al. 2009. Estimation of chlorophyll-a concentration in case II waters using MODIS and MERIS data—successes and challenges. Environmental Research Letters, 4(4): 045005

Nelson N B, Prézelin B B. 1993. Calibration of an integrating sphere for determining the absorption coefficient of scattering suspensions. Applied Optics, 32(33): 6710–6717

O'Reilly J E, Maritorena S, Mitchell B G, et al. 1998. Ocean color chlorophyll algorithms for SeaWiFS. Journal of Geophysical Research, 103(C11): 24937–24953

Pope RM, Fry E S. 1997. Absorption spectrum (380–700 nm) of pure water: II. integrating cavity measurements. Applied Optics, 36(33): 8710–8723

Röttgers R, Häse C, Doerffe R. 2007. Determination of the particulate absorption of microalgae using a point-source integrating-cavity absorption meter: verification with a photometric technique, improvements for pigment bleaching, and correction for chlorophyll fluorescence. Limnology and Oceanography: Methods, 5(Jan): 1–12

Schofield O, Grzymski J, Bissett W P, et al. 1999. Optical monitoring and forecasting systems for harmful algal blooms: possibility or pipe dream? Journal of Phycology, 35(6 suppl): 1477–1496

Sellner K G, Doucette G J, Kirkpatrick G J. 2003. Harmful algal blooms: causes, impacts and detection. Journal of Industrial Microbiology and Biotechnology, 30(7): 383–406

Shubha S, Louisa W, Emmanuel D, et al. 2004. Discrimination of diatoms from other phytoplankton using ocean-colour data. Mar Ecol Prog Ser, 272: 59–68

Stæhr P A, Cullen J J. 2003. Detection of *Karenia mikimotoi* by spectral absorption signatures. Journal of Plankton Research, 25(10): 1237–1249

Stumpf R P, Culver M E, Tester P A, et al. 2003. Monitoring *Karenia brevis* blooms in the Gulf of Mexico using satellite ocean color imagery and other data. Harmful Algae, 2(2): 147–160

Tomlinson M C, Stumpf R P, Ransibrahmanakul V, et al. 2004. Evaluation of the use of SeaWiFS imagery for detecting *Karenia brevis*—harmful algal blooms in the eastern Gulf of Mexico. Remote Sensing of Environment, 91(3–4): 293–303

Westberry T K, Siegel D A, Subramaniam A. 2005. An improved bio-optical model for the remote sensing of *Trichodesmium* spp. blooms. Journal of Geophysical Research: Oceans, 110(6): 1–11

Whitmire A L, Boss E, Cowle T J, et al. 2007. Spectral variability of the particulate backscattering ratio. Optics Express, 15(11): 7019–7031

Whitmire A L, Pegau W S, Karp-Boss L, et al. 2010. Spectral backscattering properties of marine phytoplankton cultures. Optics Express, 18(14): 15073–15093

Yentsch C S. 1962. Measurement of visible light absorption by particulate matter in the ocean. Limnology and Oceanography, 7(2): 207–217